Journal of the American Heart Association

ORIGINAL RESEARCH

Electrophysiological Characteristics of Intra-Atrial Reentrant Tachycardia in Adult Congenital Heart Disease: Implications for Catheter Ablation

Ann-Kathrin Kahle; Roberto G. Gallotti, MD; Fares-Alexander Alken, MD; Christian Meyer, MD, MA; Jeremy P. Moore, MD, MS

BACKGROUND: Ultra-high-density mapping enables detailed mechanistic analysis of atrial reentrant tachycardia but has yet to be used to assess circuit conduction velocity (CV) patterns in adults with congenital heart disease.

METHODS AND RESULTS: Circuit pathways and central isthmus CVs were calculated from consecutive ultra-high-density isochronal maps at 2 tertiary centers over a 3-year period. Circuits using anatomic versus surgical obstacles were considered separately and pathway length <50th percentile identified small circuits. CV analysis was used to derive a novel index for prediction of postablation conduction block. A total of 136 supraventricular tachycardias were studied (60% intra-atrial reentrant, 14% multiple loop). Circuits with anatomic versus surgical obstacles featured longer pathway length (119 mm; interquartile range [IQR], 80–150 versus 78 mm; IQR, 63–95; $P<0.001$), faster central isthmus CV (0.1 m/s; IQR, 0.06–0.25 versus 0.07 m/s; IQR, 0.05–0.10; $P=0.016$), faster non-isthmus CV (0.52 m/s; IQR, 0.33–0.71 versus 0.38 m/s; IQR, 0.27–0.46; $P=0.009$), and fewer slow isochrones (4; IQR, 2.3–6.8 versus 6; IQR 5–7; $P=0.008$). Both central isthmus ($R^2=0.45$; $P<0.001$) and non-isthmus CV ($R^2=0.71$; $P<0.001$) correlated with pathway length, whereas central isthmus CV <0.15 m/s was ubiquitous for small circuits. Non-isthmus CV in tachycardia correlated with CV during block validation ($R^2=0.94$; $P<0.001$) and a validation map to tachycardia conduction time ratio >85% predicted isthmus block in all cases. Over >1 year of follow-up, arrhythmia-free survival was better for homogeneous CV patterns (90% versus 57%; $P=0.04$).

CONCLUSIONS: Ultra-high-density mapping-guided CV analysis distinguishes atrial reentrant patterns in adults with congenital heart disease with surgical obstacles producing slower and smaller circuits. Very slow central isthmus CV may be essential for atrial tachycardia maintenance in small circuits, and non-isthmus conduction time in tachycardia appears to be useful for rapid assessment of postablation conduction block.

Key Words: adult congenital heart disease ■ catheter ablation ■ conduction velocity ■ high-density mapping ■ intra-atrial reentrant tachycardia

Atrial arrhythmias are commonly observed in adults with congenital heart disease (ACHD) with a lifetime cumulative incidence of 50% after reaching adulthood.[1] Historically, the increased burden of atrial arrhythmia in ACHD has been ascribed to a complex interplay of atrial dilation, arising from altered postoperative hemodynamics and atrial myocardial scar, a consequence of surgically inflicted tissue trauma with subsequent reparative fibrosis.[2] Classically, a favorable ratio of pathway length through enlarged atrial chambers and slow conduction through regions of abnormal myocardium permits

Correspondence to: Jeremy P. Moore, MD, MS, FACC, FHRS, University of California at Los Angeles (UCLA) Medical Center, Ahmanson/UCLA Adult Congenital Heart Disease Center, 100 Medical Plaza Dr, Suite 770, Los Angeles, CA 90095. E-mail: jpmoore@mednet.ucla.edu

Supplementary Material for this article is available at https://www.ahajournals.org/doi/suppl/10.1161/JAHA.121.020835

For Sources of Funding and Disclosures, see page 12.

JAHA is available at: www.ahajournals.org/journal/jaha

CLINICAL PERSPECTIVE

What Is New?

- This dual-center study demonstrates that ultra-high-density mapping has the potential to characterize conduction velocity patterns of intra-atrial reentrant tachycardias in relation to the underlying anatomical substrate in adults with congenital heart disease.
- Intra-atrial reentrant tachycardia circuit characteristics in adults with congenital heart disease vary according to clinical variables, with slower and smaller circuits for postsurgical substrates, especially those involving operations performed on the right side of the heart.

What Are the Clinical Implications?

- Very slow conduction velocity through the central isthmus appears to be a requisite for atrial tachycardia maintenance in small circuits.
- Non-isthmus conduction velocity may be more important than previously realized, with relevant implications for tachycardia cycle length, circuit size, and block validation, as conduction time around the central obstacle in tachycardia and during validation map pacing appear nearly identical.
- Intra-atrial reentrant tachycardia circuit characteristics, namely conduction velocity heterogeneity, may be associated with arrhythmia recurrence after initially successful catheter ablation.

Nonstandard Abbreviations and Acronyms

ACHD	adult congenital heart disease
CV	conduction velocity
IART	intra-atrial reentrant tachycardia
TCL	tachycardia cycle length
UHDM	ultra-high-density mapping

the maintenance of a variety of intra-atrial reentrant tachycardias (IART), so long as the resultant anatomical circuit size remains larger than the basic wavelength of the electrical wavefront.[3] To date however, the relative importance of these 2 factors, namely pathway length and conduction velocity (CV), has not been adequately assessed in ACHD, and their clinical implications remain unknown.

Recently, novel ultra-high-density mapping (UHDM) technologies have enabled rigorous elucidation of atrial arrhythmia mechanisms in ACHD.[4–7] Such technologies are able to rapidly localize protected channels of slow conduction for complex IART circuits[5] and enable comprehensive characterization of the full reentrant pathway.[6] UHDM has the potential to identify key CV patterns that could prove useful for greater understanding of the pathogenesis of IART in ACHD. Based on these considerations, it was hypothesized that circuit CV and pathway length might vary according to surgical substrate in ACHD and that an improved knowledge of these factors could facilitate catheter-based therapy for IART.

METHODS

Anonymized patient data that support the findings of this study are available from the corresponding author upon reasonable request. Consent was not obtained for data sharing, but the presented data are anonymized, and the risk of identification is minimal.

Study Design

In this dual-center study, all consecutive ACHD patients undergoing UHDM-guided catheter ablation for supraventricular tachycardia between February 2017 and September 2020 were retrospectively analyzed. All procedures were performed with the Rhythmia system (Boston Scientific, Marlborough, MA). The study was conducted in accordance with the provisions of the Declaration of Helsinki. Data collection and analysis were performed under a protocol approved by the institutional review boards of the University Heart and Vascular Center Hamburg-Eppendorf and the University of California, Los Angeles. Patients gave written informed consent before all procedures.

Procedural Protocol

All patients underwent imaging evaluation for anatomical assessment and exclusion of intracardiac thrombus. Mapping and catheter ablation were conducted under general anesthesia or deep sedation.[4] A steerable 6-F decapolar diagnostic catheter (Inquiry, 2-5-2 mm spacing; St. Jude Medical, St. Paul, MN; or Dynamic DECA, Bard Electrophysiology; Boston Scientific) was placed in the coronary sinus as a fiduciary reference. In cases without anatomic access to the coronary sinus, the catheter was placed either in the pulmonary artery or within the systemic venous atrium. If appropriate, a transbaffle puncture was performed before subsequent electrophysiology testing. For patients with an extracardiac conduit who have undergone the Fontan procedure, the needle was placed against the vena caval wall for direct cardiac puncture as previously described.[8]

The catheters consisted of an expandable, open-irrigated 64-electrode minibasket catheter (Orion; Boston Scientific) and an open-irrigated 3.5-mm tip mapping and ablation catheter (IntellaNav MiFi OI; Boston Scientific). The pulmonary venous chamber or left atrium was accessed by a transseptal puncture using a fixed curve long sheath (SL0, 8 French; St. Jude Medical) for the ablation catheter and a long steerable sheath (Zurpaz, medium curl, 8.5 French; Boston Scientific; or Agilis, 8.5 French; St. Jude Medical) for the basket catheter. Heparin was administered intravenously to maintain an activated clotting time >300 to 350 s. For patients in sinus rhythm at the beginning of the procedure, programmed stimulation with up to triple atrial extra stimuli and a minimum coupling interval of 200 ms or burst atrial pacing to a minimum cycle length of 180 ms was performed. Isoproterenol or adenosine infusion was applied as necessary.

Ultra-High-Density Mapping

UHDM was performed for all inducible tachycardias using the basket catheter. Maps were considered complete when the entire chamber anatomy was reconstructed with the best achievable electrode-tissue contact (no color gaps after assigning a fill threshold of 5 mm).[5] Basket catheter contact was assessed by progressive deflection of the sheath or catheter against the atrial wall without further catheter displacement by 3-dimensional mapping and by inspection of local electrograms. Activation maps were created under standard automatic beat acceptance criteria.[9] Wavefront propagation and activation patterns were reviewed in order to target the critical isthmus. Given reliable identification of critical isthmus sites with UHDM propagation map and global atrial histogram analysis (Lumipoint),[5,10] additional entrainment mapping was performed sparingly at the operator's discretion.

Multiple-loop tachycardias were defined as those composed of >1 independent active circuit sharing 1 common isthmus with the entire tachycardia cycle length (TCL) included in each of the circuits.[11] Dual-loop tachycardias were identified when simultaneous wavefront propagation around 2 central obstacles in opposite directions was demonstrated.[9] Single-loop IARTs were classified as continuous atrial activation, with earliest neighboring latest activation propagating around a central obstacle encompassing the entire TCL.[12] For substrate identification, a bipolar voltage <0.05 mV was considered scar and values between 0.05 and 0.5 mV as border zone, with possible individual adjustment.[5]

Catheter Ablation

Catheter ablation was performed with irrigated energy, maximum power of 40 W, and peak tip temperature of 42°C. For multiple-loop and single-loop IARTs, the practical isthmus, defined as the narrowest pathway between scars, anatomical or functional obstacles, with the least concern for collateral damage was targeted to transect the circuit by linear ablation.[12] Endpoints of previously performed ablations and connection to nonconducting structures were verified and completed, if necessary. Bidirectional block was confirmed using UHDM whenever possible.[13] Routine postprocedure testing included up to triple atrial extra stimuli using a minimum coupling interval of 180 ms and incremental atrial pacing to a minimum TCL of 200 ms. Acute, complete procedural success was defined as termination of all stable, inducible supraventricular tachycardias without catheter-induced ectopy and noninducibility of further sustained tachycardias.

Offline High-Density-Mapping Analysis

All maps were analyzed offline with the Rhythmia software using the original, unprocessed data at a single center. Only circuits with comprehensive delineation of the entire pathway were considered for the analysis. Representative offline analyses are depicted in Figure 1. The following definitions were considered for the analysis:

- *Central obstacle:* Central obstacles were "anatomic" when circumnavigating cardiac structures (such as the vena cavae, atrioventricular valve annulus, or pulmonary vein orifices) versus "surgical" when involving a prior operative substrate (eg, surgical incisions, anastomoses, plications, scarring, patch or baffle material). Identification of central obstacle(s) followed accepted definitions based on review of the congenital anatomy and operative details when available.[2]
- *Central isthmus:* The central isthmus was identified as 30% of the TCL, centered at the midpoint of the protected region of slow conduction as suggested by previous entrainment analysis in congenital heart disease.[14,15] This region was localized using UHDM[10] and was supplemented by review of the Lumipoint global activation histogram tool.[5] Central isthmus width was measured as the distance between 2 fixed or functional barriers indicated by the presence of bordering anatomical structures, dense scar consisting of areas with bipolar voltage <0.05 mV, or split potentials. Electrogram duration was measured at the anatomic midpoint of each conduction isthmus.[5]
- *Pathway length:* Pathway length was taken as the shortest distance (ie, perimeter) around the

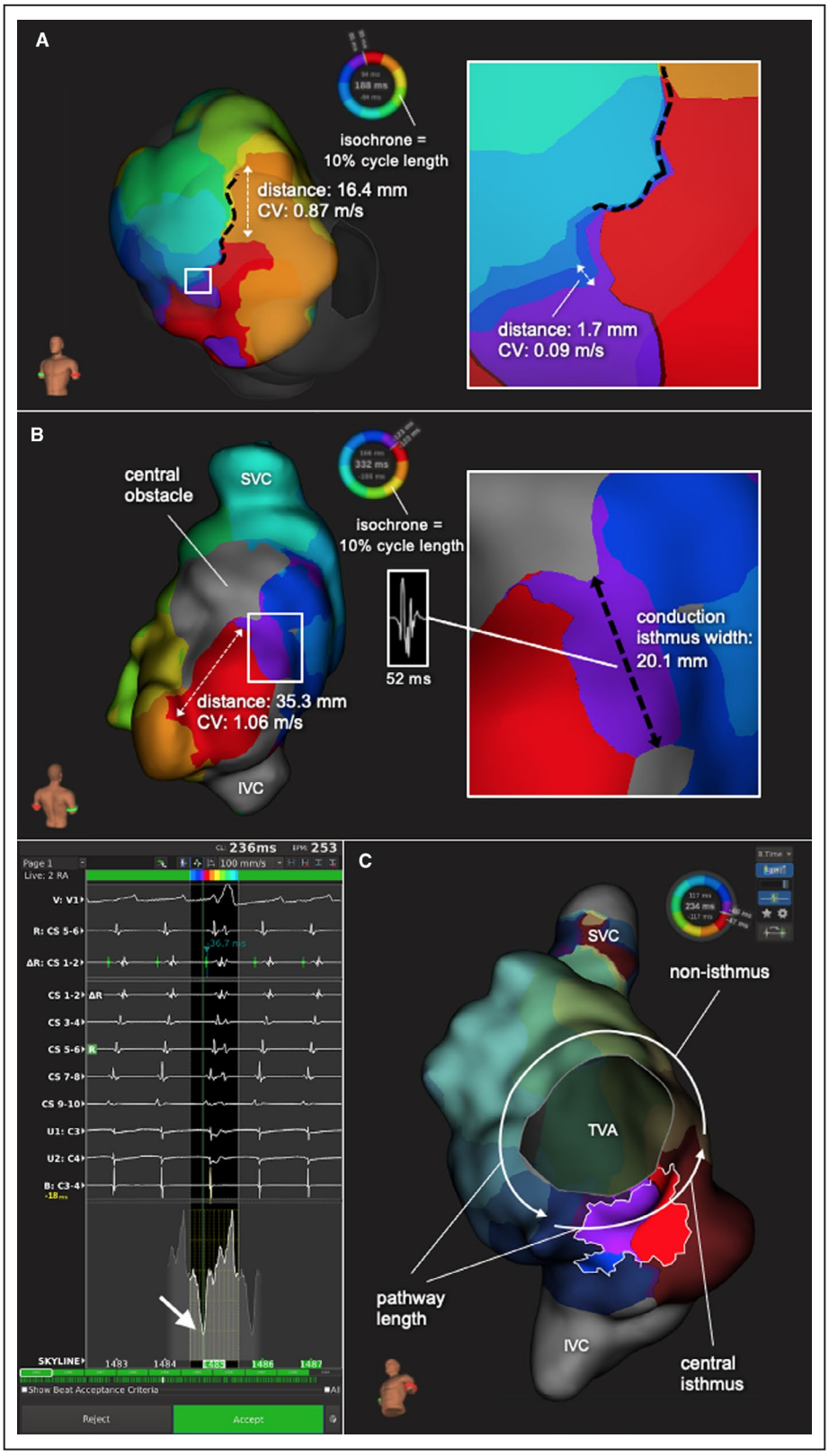

associated central obstacle.[5] For descriptive purposes, a pathway length cutoff based upon the 50th percentile was used to categorize large versus small circuits.

- *Conduction velocity:* UHDM isochronal maps consisting of 10 segments were created. The first segment was set to the central isthmus exit site and the bar distance around the central obstacle was

Figure 1. Conduction velocity analysis.
A, CV analysis of a fast tachycardia (CL 188 ms) around a functional line of block in the anterior right atrium obtained in a patient with a history of pulmonary atresia with intact ventricular septum. The patient underwent right ventricular outflow tract reconstruction and replacement of the pulmonary valve and the tricuspid annuloplasty ring. **B**, CV analysis of a slower tachycardia (CL 332 ms) around a right atrial patch in a patient after Warden procedure for partial anomalous pulmonary venous return. **C**, Cavotricuspid isthmus-dependent flutter in a patient with repaired coarctation of the aorta. CL indicates cycle length; CV, conduction velocity; IVC, inferior vena cava; SVC, superior vena cava; and TVA, tricuspid valve annulus.

measured for each isochrone. Isochronal CV was calculated as each bar distance divided by 10% of the TCL. CV was also calculated for both central isthmus and non-isthmus regions of the pathway. Slow conduction was defined as <0.3 m/s as previously suggested.[13]

- *Coefficient of variability:* The coefficient of variability was taken as the SD divided by the mean of all 10 CV values calculated in a given tachycardia circuit with greater values corresponding to more heterogeneous CV patterns. For descriptive purposes, the median value was used to classify circuits as "heterogeneous" versus "homogeneous."

After ablation, pacing was performed adjacent to all completed linear catheter ablation lesions using UHDM to verify the conduction pathway around the central obstacle and consequently conduction block through the targeted isthmus. Conduction times and velocities were recorded from all validation maps.

Follow-Up

Patients were followed every 3 to 6 months at the respective center. Pacemaker and implantable cardioverter defibrillators were interrogated through remote monitoring; 12-channel- as well as 24-hour Holter electrocardiograms were performed in all patients without implantable devices for further assessment. Recurrence was determined as any documented atrial arrhythmia lasting >30 s after a 90-day blanking period or when repeat ablation was required after initial catheter ablation. If the recurrent supraventricular tachycardia had the same origin and the TCL was in a range of ±20 ms of the index procedure's TCL, we recorded a recurrence of the original tachycardia.

Statistical Analysis

Continuous variables are presented as median (interquartile range [IQR]) and were compared by Mann-Whitney *U* test or Kruskal-Wallis test. Categorical variables are presented as counts (percentage). Associations between CV characteristics and clinical parameters were evaluated by simple linear regression for normally distributed samples. The Kaplan-Meier method was used to illustrate arrhythmia recurrence among those with and without CV heterogeneity with the log-rank test to establish statistical significance. A multivariate Cox proportional hazards model was used to investigate the effect of baseline differences on patient outcome. Baseline covariates associated with a *P* value <0.2 were included in the final multivariate model. A *P* value <0.05 was considered statistically significant. All analyses were performed using SPSS software version 25.0 (IBM SPSS Statistics, Chicago, IL).

RESULTS

Patient Population

The study included 81 patients (38.5 years [IQR, 31–55], 56% male sex) undergoing 85 procedures (Table 1).

Table. Baseline Patient and Procedural Characteristics

	n=81
Age, y	38.5 (31–55)
Male sex	45 (56)
Body mass index, kg/m^2	26 (23.4–29.1)
History of arrhythmia, y	3.6 (0.6–8.7)
Left ventricular ejection fraction, %	55 (49.5–60)
Congenital categories	
Left heart obstruction*	15 (19)
Single ventricle	15 (19)
Fontan†	12 (15)
Glenn	3 (4)
Septal defect	12 (15)
Tetralogy of Fallot variant	12 (15)
Transposition of the great arteries	8 (10)
Atrial switch procedure (Mustard/Senning)	7 (9)
Congenitally corrected	1 (1)
Ebstein's anomaly	8 (10)
Double outlet right ventricle	4 (5)
Partial anomalous pulmonary venous return	4 (5)
Other	3 (4)
Procedural and mapping data	
Procedure duration, min	202 (150–289)
Fluoroscopy duration, min	23.8 (14.6–35.8)
Radiofrequency application time, min	22.5 (13.2–38.7)
Points per map, n	11602 (7129–15622)
Time per map, min	20.0 (12.2–26.7)
Chamber volume per map, cc	136.2 (93.6–184.8)

Values are presented as median (interquartile range) or n (%).
*Aortic valve stenosis, bicuspid aortic valve, coarctation of the aorta, Shone's complex.
†Lateral tunnel Fontan in 6 patients, extracardiac in 2, Bjork in 2, intra-atrial conduit in 1, atriopulmonary in 1.

Prior cardiac surgery was performed in 94% and prior ablation in 51% of patients. The most frequent diagnoses were left heart obstruction (n=15) and single ventricle (n=15), followed by atrial or ventricular septal defect (n=12) and tetralogy of Fallot or related variant (n=12).

Procedural Characteristics

Among all 85 catheter ablation procedures, a transseptal or baffle/conduit puncture was performed in 36 (42%) cases (24 [28%] and 12 [14%], respectively). In 24 cases (28%) the systemic venous atrium or pulmonary artery was used as the fudicial reference owing to non-accessibility of the coronary sinus. Adequate contact between tissue and the basket catheter could be achieved in all patients.

Of 156 supraventricular tachycardias in total, 136 (87%) were completely mapped (mean 1.6 tachycardias per procedure) with a median TCL of 290 ms (IQR, 250–341). Tachycardia was present at procedure onset in 35 cases (41%). Tachycardia mechanisms were single-loop IART (n=82, 60%), focal (n=26, 19%), multiple-loop (n=19, 14%; dual-loop in 18), atrioventricular nodal reentrant tachycardia (n=5, 4%), atrioventricular reciprocating tachycardia (n=3, 2%) or twin atrioventricular node reentry (n=1, 1%). Tachycardias were principally targeted in the right atrium (n=107, 79%) but also in the pulmonary venous chamber or left atrium (n=21, 15%), bi-atrially (n=5, 4%) or in the coronary sinus (n=3, 2%). The median number of catheter ablation lesions resulting in termination was 3 (IQR, 1–7) with 25 of 136 (18%) tachycardias terminating with the first radiofrequency energy application. Acute, complete success was achieved in 81 cases (95%). Procedural complications are listed in Data S1.

Intra-Atrial Reentrant Circuit Parameters

The 2 most commonly observed central obstacles for single-loop IART were atriotomy in 24 (29%) and the tricuspid valve annulus in 23 (28%) cases. Dual-loop tachycardias most frequently involved a combination of the tricuspid valve annulus with an atriotomy (6 of 18 cases, 33%) or the inferior vena cava (3 of 18 cases, 17%), respectively. In 1 patient, who underwent tetralogy of Fallot repair, a multiple-loop circuit around an atriotomy, the inferior vena cava and a small scar in between, was noted (Video S1). Detailed circuit characteristics in relation to the corresponding central obstacle and underlying ACHD lesion are listed in Tables S1 and S2, respectively.

Predictors of Atrial Reentrant Circuit Characteristics

Circuit characteristics varied according to the presence of an anatomic versus surgical central obstacle. Tachycardias related to an anatomic obstacle were characterized by longer total pathway length (119.3 mm [IQR, 80.4–150.3] versus 77.7 mm [IQR, 63.1–94.7]; $P<0.001$), faster central isthmus CV (0.11 m/s [IQR, 0.06–0.24] versus 0.07 m/s [IQR, 0.05–0.10]; $P=0.016$), faster non-isthmus CV (0.52 m/s [IQR, 0.33–0.71] versus 0.38 m/s [IQR, 0.27–0.46]; $P=0.009$), fewer slow isochrones (4 [IQR, 2.3–6.8] versus 6 [IQR, 5–7]; $P=0.008$) and a smaller coefficient of variability (0.65 [IQR, 0.56–0.82] versus 0.82 [IQR, 0.69–0.92]; $P=0.004$) as compared with circuits around surgical obstacles (Figure 2 and 3). Anatomic circuit size was augmented by nearby fixed or functional block in 21 of 66 (32%) cases. Electrogram duration did not differ between groups (79.5 ms [IQR, 62–103.5] versus 88.5 ms [IQR, 72.5–104.3]; $P=0.27$).

Classification as right- versus left-sided cardiac surgery also predicted tachycardia circuit characteristics. After right heart surgery, shorter pathway length (76.3 mm [IQR, 52.8–95.2] versus 113.0 mm [IQR, 66.6–130.9]; $P=0.026$), slower central isthmus CV (0.07 m/s [IQR, 0.05–0.10] versus 0.10 m/s [IQR, 0.06–0.21]; $P=0.047$), slower non-isthmus CV (0.36 m/s [IQR, 0.25–0.47] versus 0.52 m/s [IQR, 0.28–0.60]; $P=0.036$), and more slow isochrones (6 [IQR, 5–8] versus 5 [IQR, 3.5–7]; $P=0.027$) were observed (Figure 2 and 3). Right-sided cardiac surgery was associated with nonsignificantly longer electrogram duration than left-sided surgery (95 ms [IQR, 65–107] versus 75 ms [IQR, 61–96.5]; $P=0.17$). Box plots illustrating the distribution of CVs for anatomic versus surgical and right versus left heart operations are displayed in Figure S1.

Relationship Between Conduction Velocity, Tachycardia Cycle Length, and Pathway Length

Notably, TCL was similar for circuits around anatomic versus surgical obstacles (282.5 ms [IQR, 247–320] versus 270 ms [IQR, 232.5–310]; $P=0.33$) as well as right versus left heart surgery (285 ms [IQR, 260–322] versus 280 ms [IQR, 230–317]; $P=0.63$). On the other hand, non-isthmus CV ($R^2=0.07$; $P=0.031$), but not central isthmus CV ($R^2=0.01$; $P=0.37$), correlated with TCL, with faster non-isthmus CV associated with shorter TCL. Electrogram duration correlated with central isthmus CV ($R^2=0.26$; $P<0.001$), with longer signal duration relating to slower CV.

The median pathway length for the overall population was 8.7 cm. Total pathway length was directly related to central isthmus CV ($R^2=0.45$; $P<0.001$) but with a stronger relation to non-isthmus CV ($R^2=0.71$; $P<0.001$). For small circuits (pathway length <9 cm), central isthmus CV was always <0.15 m/s whereas non-isthmus CV was always <0.5 m/s (Figure 4).

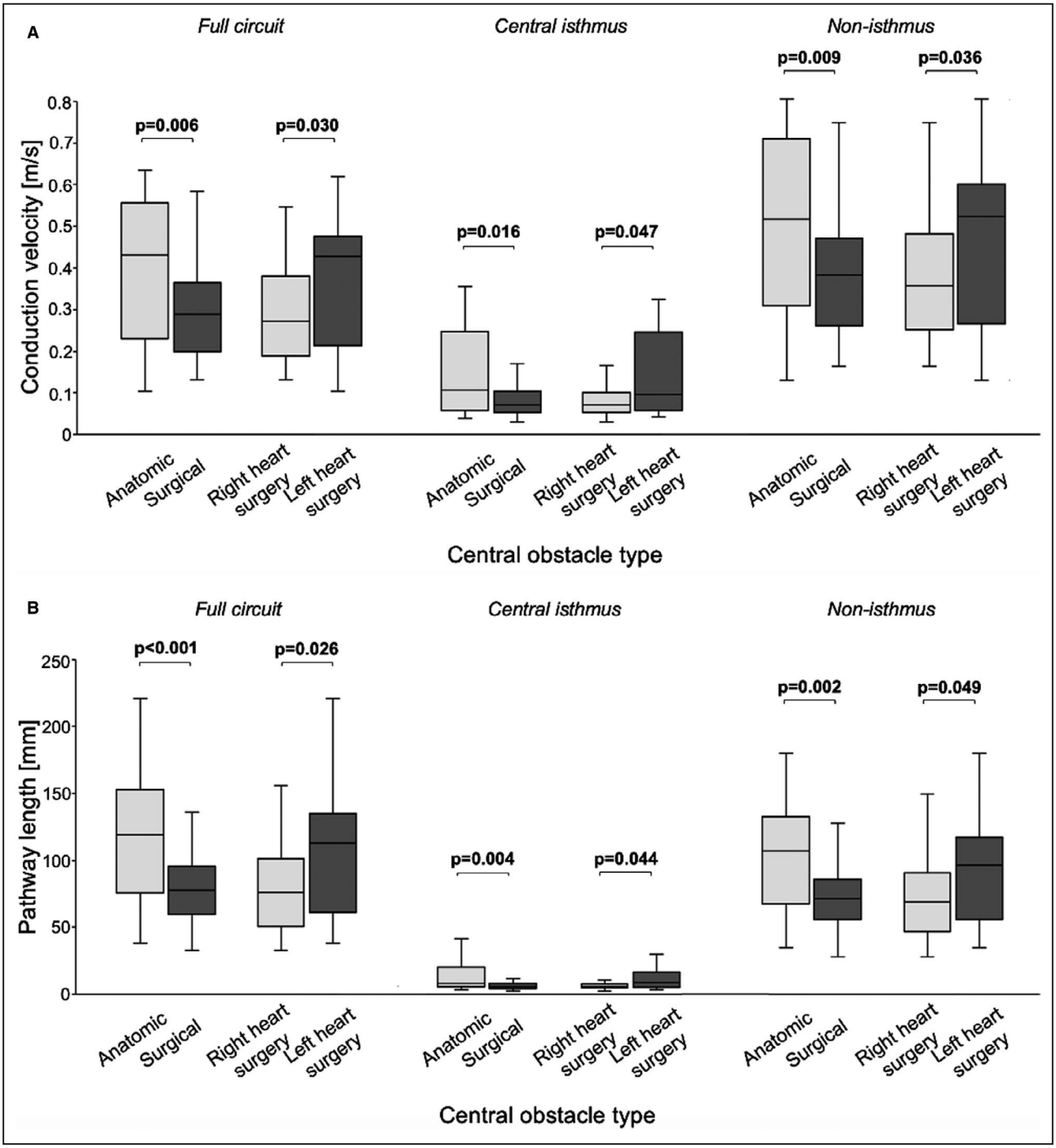

Figure 2. Circuit characteristics by type of central obstacle.
Box plots of (**A**) conduction velocity and (**B**) pathway length grouped by type of central obstacle. *P* values are based on Mann-Whitney *U* test.

Validation Map Analysis

There was a strong correlation between CV in validation maps (0.42 m/s [IQR, 0.31–0.62]) and non-isthmus CV during tachycardia (0.41 m/s [IQR, 0.28–0.64]) (β coefficient=0.9, R^2=0.94; P<0.001). Likewise, conduction time in validation maps (172.5 ms [IQR, 158.8–192.5]) and non-isthmus conduction time (185.5 ms [IQR, 161–205.6]) were nearly identical (β coefficient=0.9, R^2=0.85; P<0.001; ratio 0.94 [IQR, 0.90–0.98]). A validation map to tachycardia non-isthmus conduction time ratio >85% (range 85%–120%) was encountered in all cases of UHDM-validated isthmus block (Figure 5).

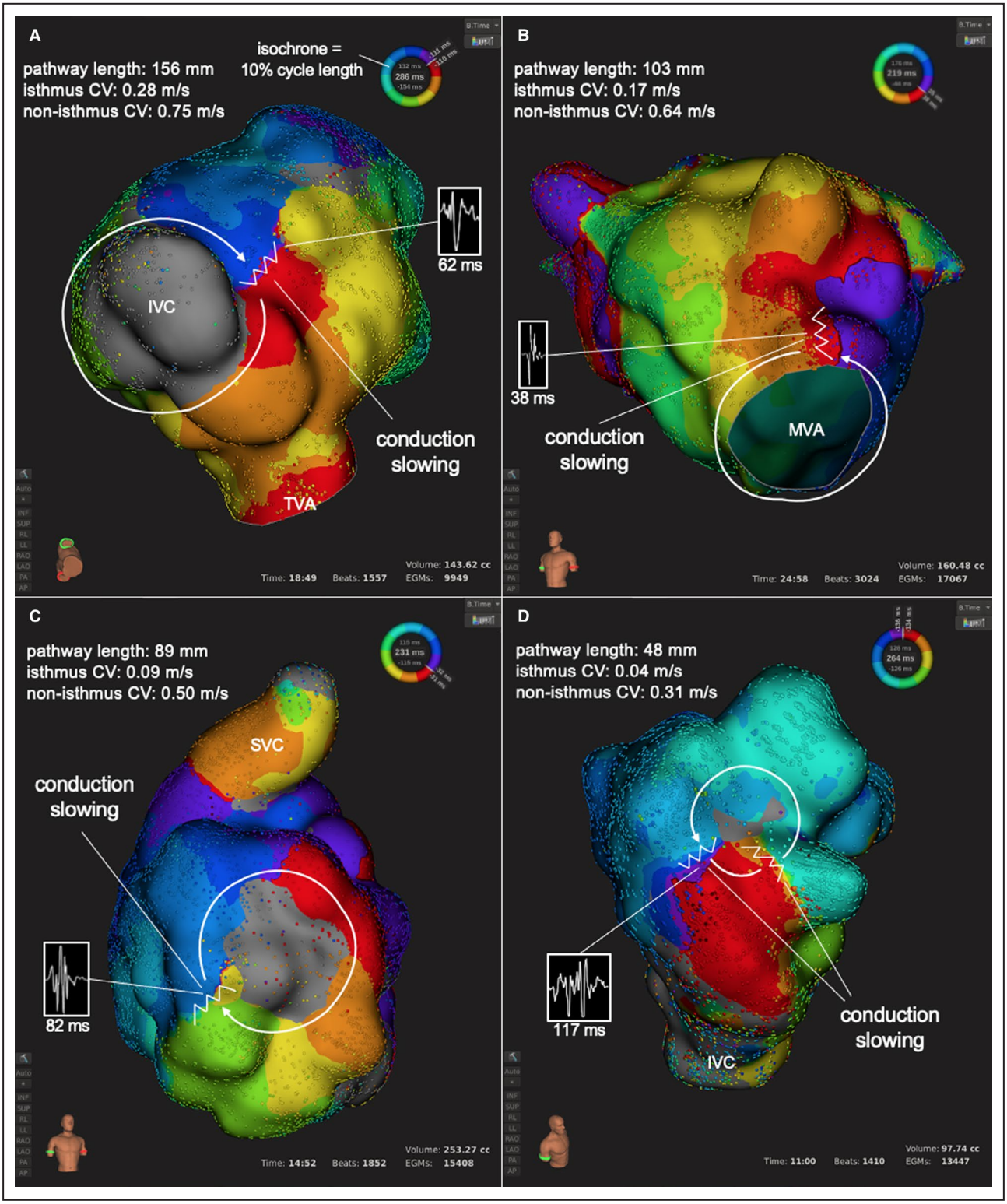

Figure 3. Representative isochronal maps depicting the major circuit subtypes.
A, Reentry around an anatomic obstacle (IVC) with minimal slowing at a single isthmus obtained in a patient with a hypoplastic right ventricle after biventricular repair with Glenn anastomosis. **B**, Perimitra flutter in a patient with Ebstein's anomaly. **C**, Reentry using an atriotomy scar obtained in a patient after atrial septal defect closure. **D**, Reentry around a postsurgical right atrial free wall scar with several regions of slowing in a patient with repaired tetralogy of Fallot. CV indicates conduction velocity; IVC, inferior vena cava; MVA, mitral valve annulus; SVC, superior vena cava; and TVA, tricuspid valve annulus.

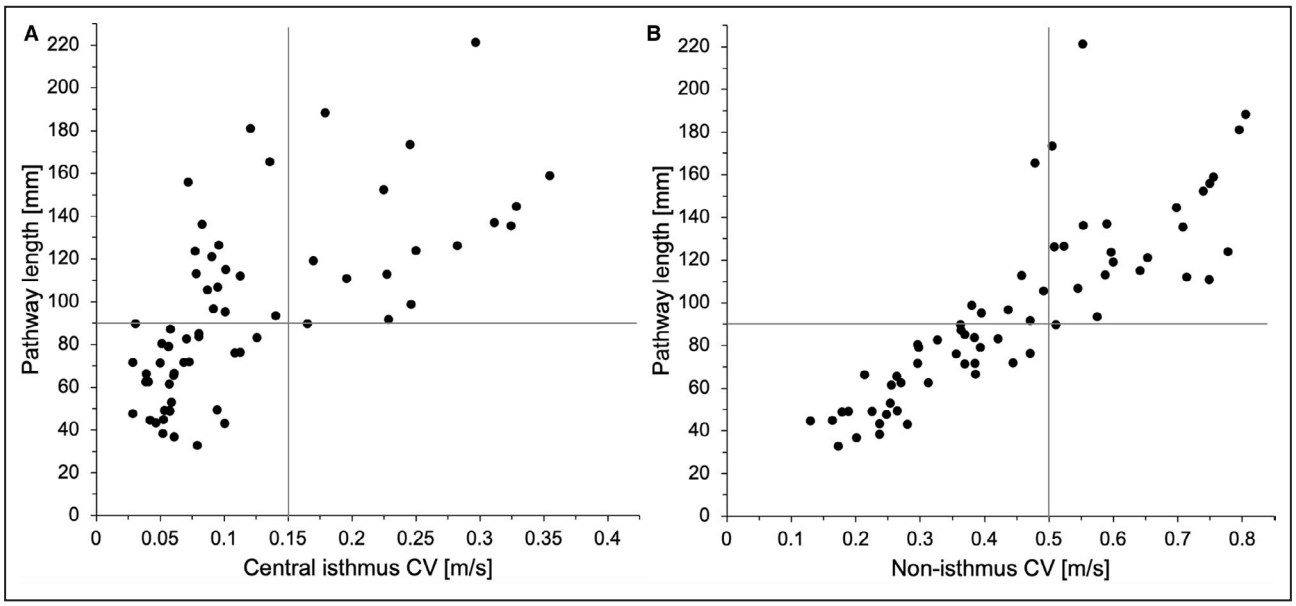

Figure 4. Association between pathway length and CV.
For small circuits (pathway length <9 cm), **(A)** central isthmus CV was always <0.15 m/s whereas **(B)** nonisthmus CV was always <0.5 m/s. CV indicates conduction velocity.

Outcome

After a median follow-up of 369 days (IQR, 224–534) 60 of 81 patients (74.1%) were free from recurrent atrial arrhythmia. Arrhythmia-free survival was better in patients presenting with tachycardias with homogeneous versus heterogeneous circuit CV (90% versus 57%;

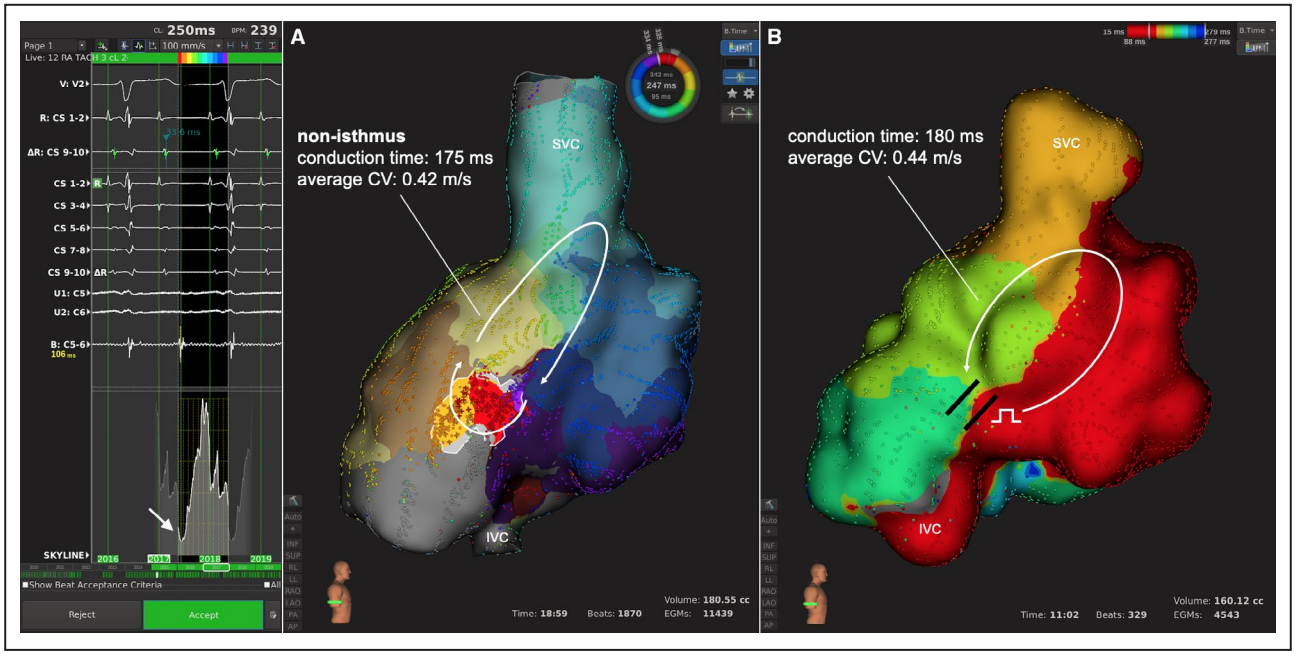

Figure 5. Validation of conduction block using conduction velocity analysis.
A, Reentry around prior Maze lesions and the SVC in a patient after Bjork Fontan for tricuspid atresia. The midpoint of the lowest global activation histogram trough is identified and the surrounding 30% of the cycle length is delimited as the central isthmus. Non-isthmus regions are defined as the remaining circuit pathway. A small gap in the Maze lesions near the IVC (corresponding to the central isthmus) was successfully targeted for ablation. **B**, Pacing just outside the central isthmus near the prior ablation lesions produces an identical conduction time as measured during tachycardia (180 vs 175 ms). Ultra-high-density mapping also confirms anterior to posterior conduction block. CV indicates conduction velocity; IVC, inferior vena cava; and SVC, superior vena cava.

P=0.038), which remained significant in multivariate analysis adjusted for age and left ventricular ejection fraction (hazard ratio, 5.9; 95% CI, 1.2–29.3; *P*=0.031) (Figure S2).

DISCUSSION

Key Findings

The present study was a large dual-center investigation of IART circuit characteristics in ACHD, aimed to characterize CV patterns in relation to the underlying anatomical substrate. Complete activation maps were available for the vast majority of cases, permitting detailed offline analysis for the major forms of congenital heart disease. The most important findings from this study are that (1) circuit characteristics varied according to clinical variables, with slower and smaller circuits for postsurgical substrates, especially those involving operations performed on the right side of the heart; (2) CV through the central isthmus appears to be associated with IART maintenance in ACHD; and (3) non-isthmus CV may be more important than previously realized, with relevant implications for TCL, circuit size, and postablation lesion assessment. Detailed exploration of these circuit characteristics in ACHD may facilitate catheter ablation and allow for improved outcomes (Figure 6).

Atrial Reentrant Circuit Characteristics in ACHD

Classically, atrial macro-reentry has been described as singular monotonous wavefront propagation around a central obstacle with 1 isolated region of slowing traditionally defined as the critical isthmus.[14] Recently however, the use of UHDM-guided systems in patients with noncongenital heart disease has indicated that more than one slowly conducting corridor might be necessary for arrhythmia maintenance in select situations (eg, after catheter ablation for atrial fibrillation).[5,13] Such studies have demonstrated regions of slow conduction at multiple points along the pathway that can enable perpetuation of small, otherwise unstable, localized circuits.

The present study suggests parallel, but unique observations in the ACHD population where postoperative scarring and other surgically acquired changes are nearly ubiquitous. In this context, distinct reentrant circuit types based on the underlying anatomic substrate were apparent, as assessed by UHDM-guided CV analysis. Conventional reentry, with a single slow conduction isthmus, was generally limited to anatomic central obstacles (such as the tricuspid valve annulus, vena cavae, or pulmonary venous orifice) and was characterized by preserved CV throughout the majority of the circuit ("non-isthmus"

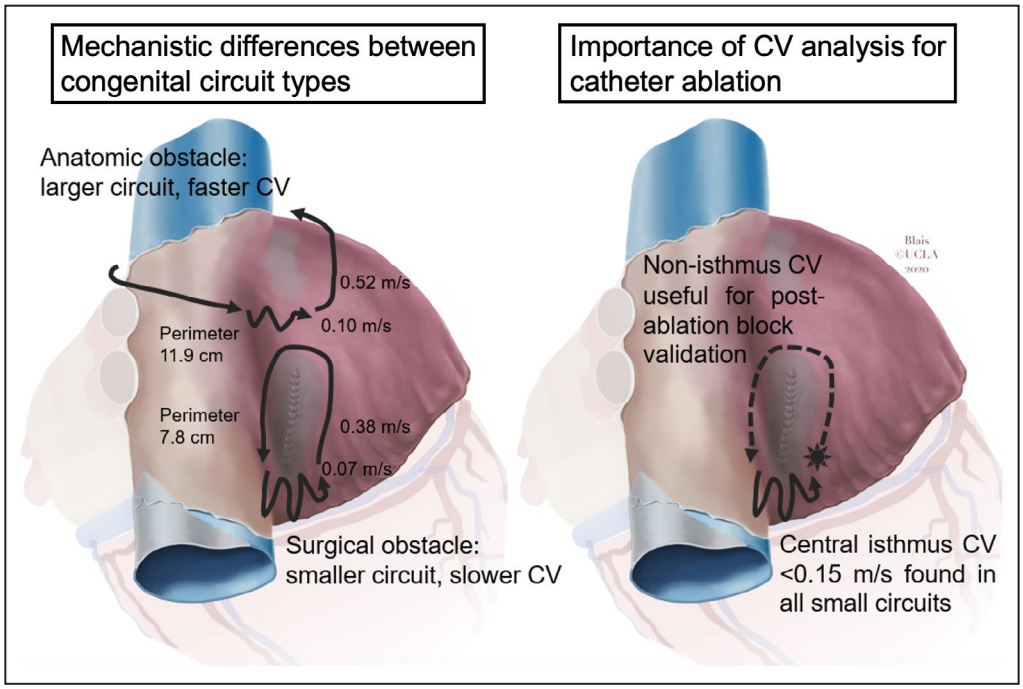

Figure 6. Summary of major findings from atrial reentry CV analysis.
Circuits with anatomic vs surgical obstacles featured longer pathway length and faster central isthmus as well as nonisthmus CV. Anatomic obstacles were augmented by nearby scar in many cases. Whereas central isthmus CV <0.15 m/s was ubiquitous for small circuits, non-isthmus CV in tachycardia was useful for block validation, as conduction time around the central obstacle in tachycardia and during validation map pacing were nearly identical. Median values are provided. CV indicates conduction velocity.

regions) that positively correlated with a longer overall pathway length. The second major circuit type, characterized by more extensive slowing in both the central isthmus and non-isthmus segments, was associated with surgical substrates (especially those after right heart operations) and exhibited shorter pathway length. These circuits often contained multiple regions of slow CV. Accordingly, CV heterogeneity, a statistical measure of deviation from the mean, was quite marked in these circuits, suggesting the interposition of both preserved and diseased conduction tissues along the tachycardia pathway. Of note, both patterns were observed to exist simultaneously in cases of dual-loop reentry, where conjoined circuits around anatomic and surgical obstacles were co-dominant despite striking differences in pathway length and CV (Figure 7).

Although we identified 2 basic atrial reentrant subtypes in this cohort, it is notable that even the "classic" form of reentry (with a single critical isthmus and faster outer loop conduction) around anatomical obstacles in ACHD appears different than that described in the noncongenital population. In our analysis, CV for atrioventricular valve-dependent IARTs was the fastest among all central obstacles (Table S1) yet was slower than formerly shown among patients unaffected by congenital heart disease.[16] This discrepancy in CV values is likely explained by substrate severity among ACHD, where atrial myopathy induced by prior surgery and postoperative hemodynamic changes is pervasive.

Clinical Implications of Conduction Velocity Analysis in ACHD

Importantly, in the present ACHD cohort CV was found to heavily influence multiple IART circuit properties. For instance, non-isthmus CV (rather than central isthmus CV) correlated strongly with TCL, suggesting that regions beyond the "critical isthmus" may play a more influential role in the maintenance of IART than previously believed. Such findings are analogous to those recently reported in rapid monomorphic ventricular tachycardia where outer loop CV alone was found to correlate with TCL.[17] Similarly, increases in both central isthmus CV and non-isthmus CV were associated with longer circuit pathway length. Moreover, very slow central isthmus conduction (<0.15 m/s) was ubiquitous among smaller circuits (defined as a central obstacle perimeter <9 cm) in the present population. This finding suggests that CV analysis could be of predictive value for substrate-based ablation in ACHD. For instance, ultra-high-density isochronal maps created during sinus rhythm or atrial pacing that identify very slow conduction corridors could potentially be used to predict stable intra-atrial reentry at the time of routine catheter ablation. This analysis could facilitate

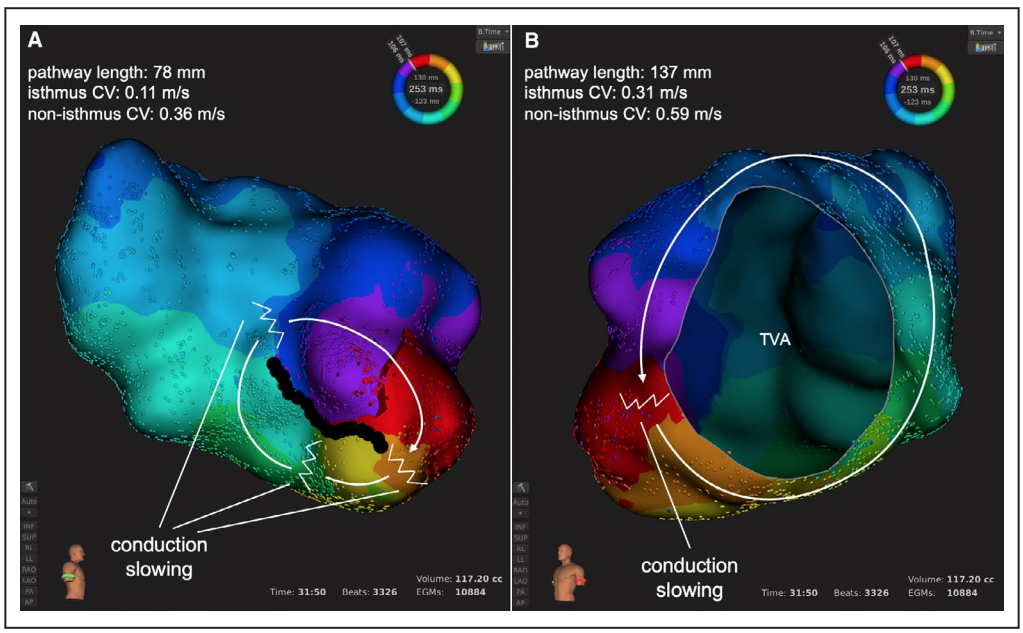

Figure 7. Dual-loop tachycardia representing both major circuit subtypes.
Dual-loop tachycardia in a patient with double outlet right ventricle and transposed great arteries. The patient underwent extracardiac Fontan operation. **A**, Reentry around a surgical atriotomy with short pathway length and multiple regions of slow CV. **B**, Reentry around the TVA with preserved CV, longer pathway length and isolated region of slowing. CV indicates conduction velocity; and TVA, tricuspid valve annulus.

empiric identification of catheter ablation targets for difficult cases in which multiple, postoperative competing tachycardias are observed and conventional activation mapping may be difficult or impossible because of nonsustained tachycardia or frequent degeneration to alternative circuits. Such a strategy warrants further, prospective study.

Finally, tachycardia CV analysis was found to predict central isthmus block with a high degree of accuracy. Importantly, non-isthmus conduction time during pacing was found to be nearly identical to the non-isthmus conduction time determined during UHDM of the active tachycardia circuit, suggesting that this interval may be a reliable reference value for assessing postablation conduction block. Identification of the anatomical boundaries of the central isthmus to localize the optimal pacing and recording sites during such block assessment was possible using UHDM and the global atrial histogram (Lumipoint) feature in this study; however, similar strategies with other mapping systems may also be feasible. Based on the present observations, postablation conduction time less than 85% of the value obtained during mapping of tachycardia would suggest that isthmus block remains incomplete and would require careful assessment for residual gaps of conduction, whereas longer values would be consistent with successful isthmus transection. Although functional slowing or even functional block could theoretically affect conduction time between active tachycardia and pacing, such differences were not apparent in the present cohort.

LIMITATIONS

The study was primarily limited by the retrospective design, relatively short follow-up, and the heterogeneity of congenital lesions and circuits. The latter limitation represents the real-world situation, however, and is expected at large volume ACHD centers. Entrainment mapping was performed only sparingly. In most cases, entrainment was not needed as activation mapping was able to characterize the entire reentrant circuit as demonstrated in our study. Therefore, it was not regularly included in our approach. Determination of CV based on 2-dimensional measurements within a 3-dimensional space is limited. Further detailed investigation of endo-epicardial circuits was not possible. All procedures were performed with the Rhythmia system so that validation with other UHDM technologies may be necessary.

CONCLUSIONS

UHDM-guided CV analysis allows identification of different reentry patterns based on the underlying surgical substrate in ACHD. Central isthmus CV is associated with tachycardia maintenance and non-isthmus CV can be useful for determination of postablation trans-isthmus conduction block. Atrial reentry circuit characteristics may be associated with arrhythmia recurrence after initially successful catheter ablation.

ARTICLE INFORMATION

Received January 18, 2021; accepted April 26, 2021.

Affiliations

Division of Cardiology, Evangelishces Krankenhaus Düsseldorf, Düsseldorf, Germany (A.K., F.A., C.M.); Institute of Neural and Sensory Physiology, Heinrich Heine University Düsseldorf, Medical Faculty, Düsseldorf, Germany (A.K., F.A., C.M.); cardiac Neuro- and Electrophysiology Research Consortium, Düsseldorf, Germany (A.K., F.A., C.M.); German Centre for Cardiovascular Research, Partner Site Hamburg/Kiel/Lübeck, Germany (A.K., F.A., C.M.); Clinic for Cardiology, University Heart & Vascular Center, University Hospital Hamburg-Eppendorf, Hamburg, Germany (A.K., F.A., C.M.); Division of Cardiology, Department of Medicine, University of California at Los Angeles Medical Center, Ahmanson University of California at Los Angeles/Adult Congenital Heart Disease Center, Los Angeles, CA (R.G.G., J.P.M.); and University of California at Los Angeles Cardiac Arrhythmia Center, University of California at Los Angeles Health System, David Geffen School of Medicine at University of California at Los Angeles, CA (J.P.M.).

Acknowledgments

We thank Lydia Merbold for technical assistance using the Rhythmia system during ablation procedures and offline analysis and Dr Benjamin Blais for preparing the summarizing illustration.

Sources of Funding

None.

Disclosures

C.M. has received fees as speaker and for participating in advisory boards from Abbott, Biosense Webster, Biotronik, and Boston Scientific. The remaining authors have no disclosures to report.

Supplementary Material

Data S1
Tables S1–S2
Figures S1–S2
Video S1

REFERENCES

1. Bouchardy J, Therrien J, Pilote L, Ionescu-Ittu R, Martucci G, Bottega N, Marelli AJ. Atrial arrhythmias in adults with congenital heart disease. *Circulation*. 2009;120:1679–1686. DOI:10.1161/CIRCULATIONAHA.109.866319.
2. Love BA, Collins KK, Walsh EP, Triedman JK. Electroanatomic characterization of conduction barriers in sinus/atrially paced rhythm and association with intra-atrial reentrant tachycardia circuits following congenital heart disease surgery. *J Cardiovasc Electrophysiol*. 2001;12:17–25. DOI:10.1046/j.1540-8167.2001.00017.x.
3. Waldo AL. Atrial flutter. New directions in management and mechanism. *Circulation*. 1990;81:1142–1143. DOI:10.1161/01.CIR.81.3.1142.
4. Alken F-A, Klatt N, Muenkler P, Scherschel K, Jungen C, Oezge Akbulak R, Kahle A-K, Gunawardene M, Jularic M, Dinshaw L, et al. Advanced mapping strategies for ablation therapy in adults with congenital heart disease. *Cardiovasc Diagn Ther*. 2019;9:S247–S263. DOI:10.21037/cdt.2019.10.02.
5. Moore JP, Buch E, Gallotti RG, Shannon KM. Ultrahigh-density mapping supplemented with global chamber activation identifies noncavotricuspid-dependent intra-atrial re-entry conduction isthmuses in adult congenital heart disease. *J Cardiovasc Electrophysiol*. 2019;30:2797–2805. DOI:10.1111/jce.14251.

6. Martin CA, Yue A, Martin R, Claridge S, Sawhney V, Maury P, Lowe M, Combes N, Heck P, Begley D, et al. Ultra-high-density activation mapping to aid isthmus identification of atrial tachycardias in congenital heart disease. *JACC Clin Electrophysiol*. 2019;5:1459–1472. DOI:10.1016/j.jacep.2019.08.001.
7. Alken FA, Chen S, Masjedi M, Purerfellner H, Maury P, Martin CA, Sacher F, Jais P, Meyer C. Basket catheter-guided ultra-high-density mapping of cardiac arrhythmias: a systematic review and meta-analysis. *Future Cardiol*. 2020;16:735–751. DOI:10.2217/fca-2020-0032.
8. Moore JP, Gallotti RG, Tran E, Perens GS, Shannon KM. Ten-year outcomes of transcaval cardiac puncture for catheter ablation after extracardiac Fontan surgery. *Heart Rhythm*. 2020;17:1752–1758. DOI:10.1016/j.hrthm.2020.05.007.
9. Mantziari L, Butcher C, Shi R, Kontogeorgis A, Opel A, Chen Z, Haldar S, Panikker S, Hussain W, Jones DG, et al. Characterization of the mechanism and substrate of atrial tachycardia using ultra-high-density mapping in adults with congenital heart disease: impact on clinical outcomes. *J Am Heart Assoc*. 2019;8:e010535. DOI: 10.1161/JAHA.118.010535.
10. Latcu DG, Bun SS, Viera F, Delassi T, El Jamili M, Al Amoura A, Saoudi N. Selection of critical isthmus in scar-related atrial tachycardia using a new automated ultrahigh resolution mapping system. *Circ Arrhythm Electrophysiol*. 2017;10:e004510. DOI: 10.1161/CIRCEP.116.004510.
11. Takigawa M, Derval N, Martin CA, Vlachos K, Denis A, Kitamura T, Cheniti G, Bourier F, Lam A, Martin R, et al. A simple mechanism underlying the behavior of reentrant atrial tachycardia during ablation. *Heart Rhythm*. 2019;16:553–561. DOI: 10.1016/j.hrthm.2018.10.031.
12. Takigawa M, Derval N, Frontera A, Martin R, Yamashita S, Cheniti G, Vlachos K, Thompson N, Kitamura T, Wolf M, et al. Revisiting anatomic macroreentrant tachycardia after atrial fibrillation ablation using ultrahigh-resolution mapping: implications for ablation. *Heart Rhythm*. 2018;15:326–333. DOI: 10.1016/j.hrthm.2017.10.029.
13. Frontera A, Mahajan R, Dallet C, Vlachos K, Kitamura T, Takigawa M, Cheniti G, Martin C, Duchateau J, Lam A, et al. Characterizing localized reentry with high-resolution mapping: evidence for multiple slow conducting isthmuses within the circuit. *Heart Rhythm*. 2019;16:679–685. DOI: 10.1016/j.hrthm.2018.11.027.
14. Nakagawa H, Shah N, Matsudaira K, Overholt E, Chandrasekaran K, Beckman KJ, Spector P, Calame JD, Rao A, Hasdemir C, et al. Characterization of reentrant circuit in macroreentrant right atrial tachycardia after surgical repair of congenital heart disease: isolated channels between scars allow "focal" ablation. *Circulation*. 2001;103:699–709. DOI: 10.1161/01.cir.103.5.699.
15. Lesh MD, Kalman JM, Saxon LA, Dorostkar PC. Electrophysiology of "incisional" reentrant atrial tachycardia complicating surgery for congenital heart disease. *Pacing Clin Electrophysiol*. 1997;20:2107–2111. DOI: 10.1111/j.1540-8159.1997.tb03638.x.
16. Itoh T, Kimura M, Sasaki S, Owada S, Horiuchi D, Sasaki K, Ishida Y, Takahiko K, Okumura K. High correlation of estimated local conduction velocity with natural logarithm of bipolar electrogram amplitude in the reentry circuit of atrial flutter. *J Cardiovasc Electrophysiol*. 2014;25:387–394. DOI: 10.1111/jce.12329.
17. Nishimura T, Upadhyay GA, Aziz ZA, Beaser AD, Shatz DY, Nayak HM, Tung R. Circuit determinants of ventricular tachycardia cycle length: Characterization of fast and unstable human ventricular tachycardia. *Circulation*. 2021;143:212–226. DOI: 10.1161/CIRCULATIONAHA.120.050363.

SUPPLEMENTAL MATERIAL

Data S1.

Procedural complications

~~A~~mong all 85 procedures the following complications (n=7, 8.2%), each in one patient, occurred: cerebral embolic event with post-procedural diplopia and minimal sequela at last follow-up, small pericardial effusion, ventricular lead micro-dislodgement, peri-procedural transient atrioventricular block, peri-procedural diffuse erythematous rash leading to loss of fidelity of previously constructed maps, retroperitoneal venous bleeding and arterial dissection. All complications resolved spontaneously without the need for intervention.

Table S1. Circuit characteristics of reentry tachycardias according to their central obstacle

Variable	ASD patch/ device (n=6)	Atriotomy (n=22)	AV valve (n=17)	Crista terminalis (n=3)	Free wall scar (n=2)	Pulmonary veins/ridge (n=5)	Surgical baffle (n=4)	Vena cava (n=5)	*p* value
Cycle length, mm	250 (232.5-260)	275 (247-319)	270 (250-314)	350 (335-380)	257.5 (243.8-271.3)	270 (210-280)	295 (247.5-333)	285 (240-305)	.314
Pathway length, mm	82.2 (50.2-97.3)	77.5 (65.6-93.8)	135.4 (112.8-158.8)	78.9 (72.5-83.0)	87.6 (85.6-89.6)	62.5 (44.5-123.5)	61.9 (46.7-91.3)	115.1 (49.2-155.7)	.003
Isthmus width, mm	13.4 (12.5-18.8)	15.6 (13.7-19.3)	18.1 (15.6-20.6)	16.6. (15.2-21.0)	15.8 (15.5-16.1)	10.9 (8.6-19.2)	13.2 (6.8-19.6)	10.1 (8.0-17.4)	.591
Signal duration, ms	77.5 (63.5-87)	84.5 (72-104.3)	62 (57-75)	148 (117.5-164)	124 (99.5-148.5)	97 (87-102)	107 (98.8-114.8)	93 (84-104)	.014
Average CV, m/s	0.31 (0.20-0.39)	0.29 (0.21-0.33)	0.44 (0.40-0.59)	0.23 (0.19-0.25)	0.35 (0.32-0.37)	0.23 (0.18-0.44)	0.27 (0.17-0.38)	0.48 (0.21-0.55)	.015
Slowest CV, m/s	0.06 (0.04-0.10)	0.06 (0.04-0.08)	0.15 (0.10-0.23)	0.0378 (0.0376-0.0446)	0.08 (0.08-0.09)	0.05 (0.04-0.06)	0.05 (0.04-0.07)	0.07 (0.06-0.07)	.004
Fastest CV, m/s	0.66 (0.58-0.89)	0.70 (0.59-0.84)	0.86 (0.78-1.15)	0.52 (0.52-0.72)	0.72 (0.68-0.77)	0.51 (0.47-1.09)	0.96 (0.77-1.04)	0.98 (0.51-1.25)	.493
Isthmus CV, m/s	0.08 (0.08-0.13)	0.07 (0.06-0.09)	0.22 (0.11-0.30)	0.06 (0.05-0.06)	0.15 (0.12-0.19)	0.05 (0.04-0.08)	0.07 (0.05-0.09)	0.09 (0.07-0.10)	.001
Non-isthmus CV, m/s	0.37 (0.14-0.50)	0.37 (0.28-0.43)	0.55 (0.50-0.71)	0.30 (0.26-0.33)	0.43 (0.41-0.45)	0.31 (0.24-0.60)	0.36 (0.23-0.49)	0.64 (0.27-0.75)	.035
Coefficient of variability	0.84 (0.64-0.95)	0.82 (0.71-0.90)	0.58 (0.39-0.65)	0.97 (0.90-1.00)	0.63 (0.50-0.76)	0.84 (0.74-0.85)	0.86 (0.77-1.09)	0.69 (0.68-0.75)	.002
Slow isochrones, n	5.5 (5-6.8)	6 (5.3-7)	4 (2-5)	7 (6.5-7.5)	4.5 (3.3-5.8)	7 (5-7)	6.5 (5-8.3)	4 (4-7)	.008
Circuit length associated with slow CV, %	26.7 (18.5-35.8)	28.2 (15.6-32.7)	13.4 (6.4-22.8)	34.9 (26.2-40.0)	20.4 (13.7-27.2)	33.8 (12.9-40.8)	31.8 (19.0-43.5)	11.8 (8.7-36.4)	.155

Values are presented as median (IQR).

ASD, atrial septal defect; AV, atrioventricular; CV, conduction velocity

p values based on the Kruskall-Wallis test.

Table S2. Procedural and circuit characteristics by congenital heart disease subgroup

Variable	ASD (n=10)	D-TGA (n=2)	Fontan (n=9)	LVOTO (n=8)	TOF (n=7)	*p* value
Age, y	54 (50.8-65)	36.5 (36.3-36.8)	35 (32-39)	58.5 (46.3-66)	48 (31.5-57)	.095
Cycle length, ms	235 (226.3-296)	250 (210-290)	270 (250-291.3)	305 (246-335)	310 (280-322)	.231
Pathway length, mm	82.5 (58.4-120.1)	104.4 (91.6-112.2)	93.4 (83.0-116.6)	130.9 (81.6-166.2)	62.4 (49.0-66.1)	.069
Isthmus width, mm	15.6 (13.6-21.3)	11.3 (7.1-15.6)	15.8 (13.1-18.2)	17.3 (16.4-20.6)	14.9 (13.4-16.6)	.298
Signal duration, ms	73 (62-88)	82.5 (63-100.5)	78.5 (65.8-94.3)	87.5 (66.8-110.3)	98 (65-117)	.532
Average CV, m/s	0.34 (0.21-0.45)	0.38 (0.36-0.43)	0.35 (0.28-0.49)	0.41 (0.27-0.59)	0.20 (0.18-0.20)	.036
Slowest CV, m/s	0.07 (0.05-0.11)	0.10 (0.09-0.11)	0.08 (0.06-0.09)	0.07 (0.05-0.15)	0.05 (0.04-0.05)	.062
Fastest CV, m/s	0.83 (0.57-0.94)	0.84 (0.75-0.96)	0.69 (0.62-1.12)	0.88 (0.62-1.13)	0.79 (0.51-0.81)	.672
Isthmus CV, m/s	0.09 (0.06-0.19)	0.11 (0.11-0.14)	0.10 (0.08-0.14)	0.11 (0.06-0.23)	0.06 (0.05-0.06)	.071
Non-isthmus CV, m/s	0.42 (0.26-0.58)	0.46 (0.45-53)	0.45 (0.37-0.64)	0.51 (0.37-0.71)	0.25 (0.23-0.27)	.035
Coefficient of variability	0.80 (0.58-0.90)	0.66 (0.58-0.69)	0.67 (0.59-0.82)	0.67 (0.59-0.75)	0.97 (0.90-1.30)	.019
Slow isochrones, n	5.5 (3.5-7)	5 (4.5-5.3)	5.5 (4-6)	4 (3.3-5.8)	8 (7-8)	.053
Circuit length associated with slow CV, %	20.7 (12.5-36.9)	24.5 (16.9-29.5)	20.8 (8.6-33.2)	14.7 (10.5-27.8)	32.5 (27.7-43.1)	.372
Fluoroscopy duration, min	18.3 (14.3-28.7)	41.9 (41.5-42.4)	42.9 (28.2-51.7)	31.2 (20.6-34.7)	17.5 (11.8-22.4)	.056
Radiofrequency applications, n	24 (19-41)	55 (55-55)	39.5 (29.5-84.8)	34 (20.3-48)	20 (11-25)	.234
Radiofrequency application time, min	17.4 (10.6-34.7)	43.2 (41.0-45.4)	35.4 (25.8-67.8)	19.1 (17.7-32.5)	19.4 (17.2-31.9)	.279

Values are presented as median (IQR).

ASD, atrial septal defect; CV, conduction velocity; D-TGA, d-transposition of the great arteries; LVOTO, left ventricular outflow tract obstruction; TOF, Tetralogy of Fallot

p values based on the Kruskall-Wallis test.

Figure S1. Conduction velocity dispersion.

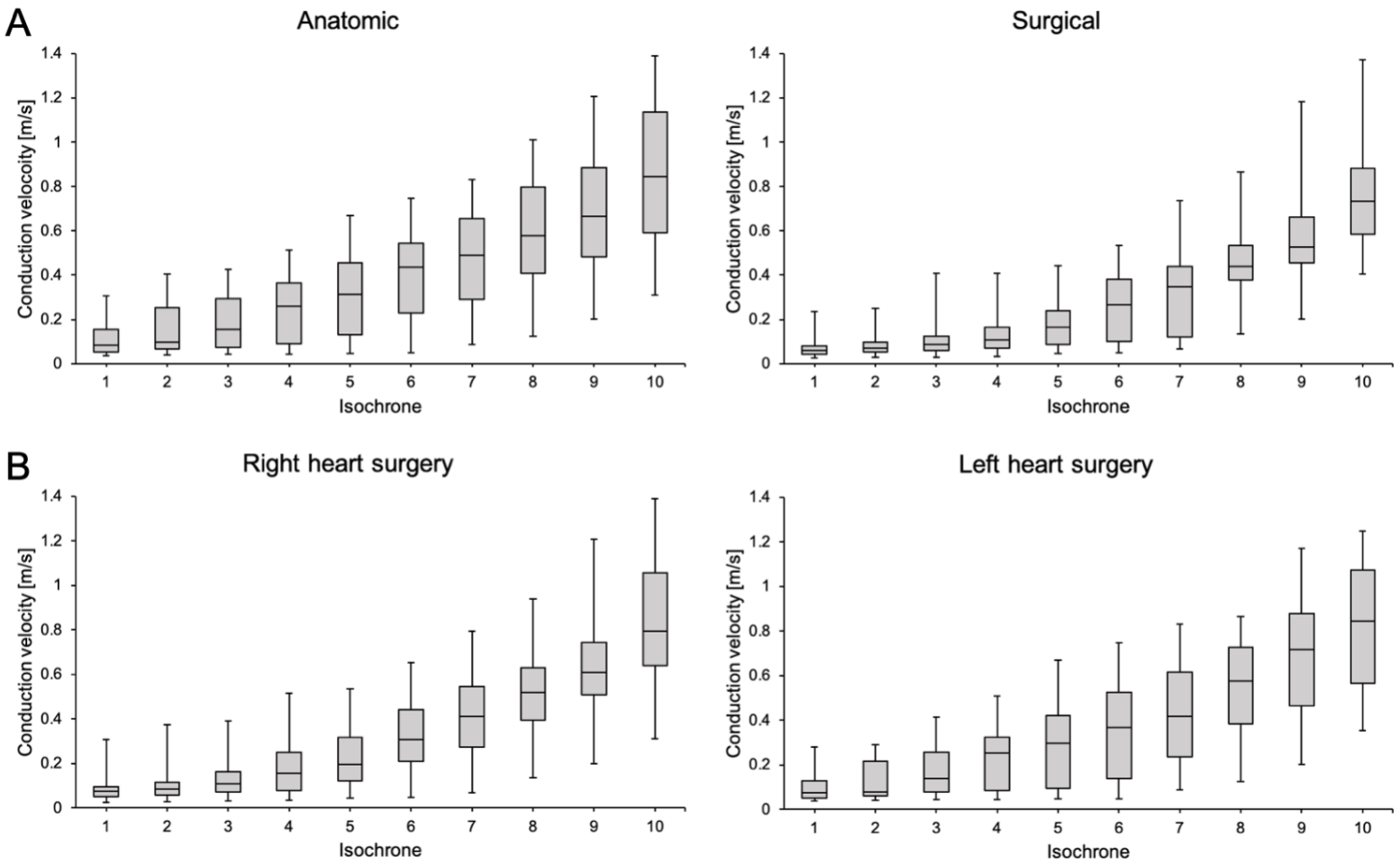

Box plots of conduction velocity dispersion grouped by central obstacle. Panel A, anatomic and surgical obstacles and Panel B, right and left heart surgery. Values are arranged from slowest to fastest irrespective of location within the circuit.

Figure S2. Patient outcome after a single ablation procedure.

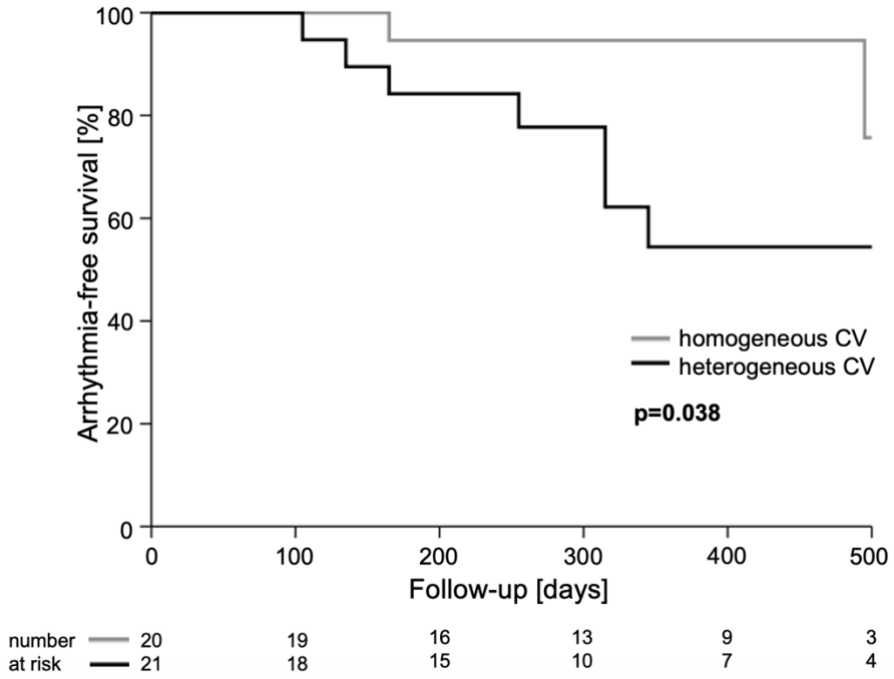

Kaplan-Meier curve illustrating arrhythmia-free survival for patients with homogeneous vs heterogenous circuit CV (*p* value based on the log-rank test). Patients with both types of circuits were excluded from this analysis.

CV, conduction velocity

Supplemental Video Legend:

Video S1. Multiple-loop tachycardia in a patient with Tetralogy of Fallot repair

Video clip demonstrating circuits around a surgical atriotomy, the inferior vena cava, and a small scar in between. Best viewed with Windows Media Player.